



1-Naphthol removal by Fenton-like heterogenous photocatalysis: Kinetic modelling, optimization, and prediction by response surface methodology

Hiu Lam So, Wei Chu*

Department of Civil and Environmental Engineering, The Hong Kong Polytechnic University, Hung Hom, Kowloon, Hong Kong

ARTICLE INFO

Keywords:

Advanced oxidation processes
Prediction model
Multiple regression
Response surface analysis
Process optimization
Peroxymonosulfate
Column reactor
Iron hydroxide

ABSTRACT

Degradation of 1-Naphthol by combined photocatalysis and adsorption in column reactor was studied, and the performance could be predicted by employing a proposed multiple regression model. The model includes four variables: concentration of 1-Naphthol, concentration of peroxymonosulfate (PMS), FeOOH dosage and pH, along with their second-order effects and interactions. Statistical analyses were performed to verify the statistical significance of the regressors, and extra experimental sets were conducted to validate the proposed model. The mathematical model proposed exhibited good reproducibility with no significant statistical difference between the experimental and predicted values. Response surface methodology was used to explore the relationship between the four variables and the response. The process optimal ranges can be further refined at pH 2–2.5; [PMS] = 1.2–1.4 mM; and FeOOH 2.75–3 g respectively, according to the proposed overlaid contour plots.

1. Introduction

Water pollution by polycyclic aromatic hydrocarbon (PAH) especially from the discharge of chemical industries is of great concern. 1-naphthol (1-Na) is a top listed priority contaminant by European Union and US EPA [1,2]. 1-Na is commonly used in the production of dyes, plastics and insecticides [3] and is frequently detected in wastewater [4]. Previous reports have shown that 1-Na is an endocrine disruptor, affecting the reproductive hormone in male [5]. It is also found to be carcinogenic at the concentration as low as 0.1 mM [6]. Similar to other PAHs, 1-Na is hardly biodegradable unless in specialized environments [1], and the degradation of 1-Na relies on mainly the physical and/or chemical processes.

In the past, the removal of polycyclic organics was commonly conducted by adsorption [2,7]. Various adsorbents have been developed including polymers and nanomaterials etc., however, the common drawbacks are the extensive retention time required for the process to reach equilibrium, and the regeneration of the spent adsorbents is energy intensive [8–13]. Adsorption was therefore not widely used in practice. A synthesis of physiochemical process is therefore adopted in this study to remove 1-Na present in wastewater. This system combines advanced oxidation process (AOP) and adsorption to enhance the removal of 1-Na and to compromise the drawbacks as mentioned above. A study has examined a similar process using Fe₃O₄ and it was efficient

in removing PAHs in water [14]. In this study, FeOOH was chosen to be the adsorbent/catalyst. Previous studies have discovered the assistive role of FeOOH in degrading organics, providing promising results [15–17]. FeOOH together with UV-C, was used to assist the activation of Peroxymonosulfate (PMS) to generate sulfate radicals (SO₄^{•-}) and hydroxyl radicals (•OH) as powerful oxidants to oxidize organic pollutants into carbon dioxide and water as final products [18,19]. To accommodate the dual role of catalyst as well as adsorbent, a unique column reactor was designed, such that simultaneous adsorption and advanced oxidation could be facilitated.

In full scale wastewater treatment plants, precise prediction of the reactor performance is vital. In this case, a mathematical modeling technique, multiple regression between a dependent variable and various independent variables, was proposed and verified to provide promising and accurate prediction. Analogous prediction models were used previously for the prediction of contaminant formation in drinking water [20,21]. Yet, studies on the prediction of treatment capacity of an advanced oxidation process in column reactor is very limited.

The aims of this paper were to (1) examine and develop suitable kinetic model in terms of the removal rate; (2) select a mathematical model to predict the removal of 1-Na under this simultaneous AOP and adsorption process in the specialized reactor; (3) optimize the process parameter mathematically, and (4) provide guidance for the proposed treatment process for the real applications.

* Corresponding author.

E-mail address: cwchu@polyu.edu.hk (W. Chu).

<https://doi.org/10.1016/j.cej.2022.100395>

2. Materials and methods

2.1. Chemicals and reagents

1-Napathol (C₁₀H₉O, CAS 90–15–3) was purchased from Aladdin. Peroxymonosulfate compound (KHSO₅ · 0.5KHSO₄ · 0.5K₂SO₄, CAS70693–62–8) and Iron (III) oxide (FeOOH 30–50 mesh, CAS20344–49–4) were purchased from Sigma-Aldrich Inc., USA. H₂SO₄ and NaOH were used for pH adjustment. All solutions were prepared using 18.2 MΩ cm distilled-deionized water from Bamstead NANO pure water system (Thermo Fisher Scientific Inc., USA). The acetonitrile for mobile phase was LC-MS grade and purchased from Tedia Company, USA.

2.2. Experimental setup for data collection

A glass column reactor (74 mm internal diameter x 500 mm height) was custom made, in which a peristaltic pump was used to control the flow rate into the column from the top, producing a downward flow by gravity. The experimental setup is shown in Fig. S1. A submersible Philips lamp (TUV-11 W G11 T5, 253.7 nm, 36 cm length) was used as UV source and was submerged inside the column. The catalyst bed was prepared by packing the catalysts into quartz bead (3.35–4.75 mm diameter) and placed into the reactor in contact with the whole UV lamp. The volume of reaction mixture is maintained at 300 mL throughout the experiment, in which the influent flowrate and effluent flowrate was controlled by the peristaltic pump and by a valve, respectively. Samples were collected through the valve and were quenched by methanol before analysis. Prior the experiment, 300 mL of distilled water was used to fill the reactor to ensure a stable flow pattern during the experiment. All experiments were repeated for less than 5% error.

2.3. Quantification of 1-Na and identification of intermediate products

The remaining [1-Na] in solution was quantified by a Dionex Ultimate 3000 Ultra High Pressure Liquid Chromatography (UHPLC) with Thermo Hypersil GOLD column (1.9 μm, 50 × 2.1 mm); and a Thermo Scientific UV/vis detector was set at 295 nm for detection. The mobile phase was a mixture of acetonitrile and water at 60:40 (v/v). The flow rate and injection volume were 0.2 mL min⁻¹ and 10 μL, respectively.

The oxidation products were identified using Agilent 7890B GC with 5977B Mass Selective Detector (GC/MS) and the abovementioned UHPLC with Bruker amaZon SL ESI Quadrupole Mass Spectrometer (LC/MS). The column temperature for GC/MS is programmed as: 35 °C for 2 min, then increased to 150 at 5 °C min⁻¹, and held for 10 min; then raised to 300 at 10 °C min⁻¹ and held for another 10 min. The mobile phase for LC/MS consists of (A) acetonitrile and (B) distilled water and the gradient is as follows: (1) 90% of B was kept during first 2 min; (2) A was increased from 10% to 90% from 2–20 min and held for 10 min; (3) the ratio is returned to initial at 30–35 min.

2.4. Model calibration and statistical analysis

The regression and statistical analysis for all variables was performed by SPSS software from IBM. Among all the factors affecting the removal rate of a Fenton-like process, five were chosen to be included in this study ([1-Na], FeOOH, [PMS], pH and Retention time), where other parameters were kept constant. The figures were plotted using a self-prepared program in MATLAB software. Three dimensional plots and their respective contour plots were analyzed to examine the interaction effects and optimization was conducted based on the overlaid contour plots.

2.5. Validation of multiple regression models

To validate the developed multiple regression models, another twelve sets of experiments were conducted for this purpose. The R² was obtained to estimate fittings between the experimental and predicted values. Then, a T-test is used to calculate t_{value} of the model predictions, the difference between experimental and predicted values was determined by comparing the t_{value} with t_{critical}. If t_{value} < t_{critical}, the difference would be considered insignificant.

3. Results and discussions

3.1. Kinetic model for 1-Na degradation

As the column was filled with 300 mL of distilled water before the start of reaction for flow equalization, the reaction mixture requires 20 min (Tank volume/Pumping flowrate) to purge out the distilled water in the column and be collected at outlet. Hence, the samples are ready to be collected after 20 min of pumping. The plot remaining concentration in the system vs *t* exhibits a concave curve shape, where an exponential growth was observed between 20–30 min and leveled off towards the end of reaction. To better describe the trend of the reaction curve, the following equation is proposed.

$$\frac{C}{C_0} = \frac{t}{a + bt} \quad (1)$$

Where *C* is the concentration of 1-Na remaining in the system after reaction time *t* (min), *C*₀ is the initial 1-Na concentration. *a* and *b* are two mathematical constants. Eq. (1) can be linearized into Eq. (2), and the constants become solvable.

$$t/(C/C_0) = a + bt \quad (2)$$

The constants *a* (intercept) and *b* (slope) are obtained by plotting a straight line *t* / (*C*/*C*₀) against *t*, in which the span rate of the reaction (rate to reach to the end) could be determined by differentiating *C*_{*t*}/*C*₀ with respect to *t*

$$\frac{dC_t/C_0}{dt} = \frac{d}{dt} \left(\frac{t}{a + bt} \right) \quad (3)$$

$$= \frac{a}{(a + bt)^2} \quad (4)$$

the initial reaction rate *k*_{*i*} therefore could be estimated when *t* approaches 0 (Eq. (5)). As all of the reaction appeared to level off towards the end of reaction, calculating the rate of reaction for the later stage is less meaningful, instead, the initial rate, *k*_{*i*} = $\frac{1}{a}$ (min⁻¹), could be useful to distinguish the performance of different reaction conditions.

$$\lim_{t \rightarrow 0} \frac{a}{(a + bt)^2} = \frac{1}{a} \quad (5)$$

The maximum treatment capacity of the system could be estimated by the *C*/*C*₀ at time approaches infinity (*t* → ∞). As *t* approaches infinity, *a* could be neglected as it is very small compared to *bt*_∞, such that $\lim_{t \rightarrow \infty} \frac{C}{C_0}$ could be rewritten as 1/*b* (dimensionless), and the removal is represented by 1–1/*b*.

$$\lim_{t \rightarrow \infty} \frac{C}{C_0} = \frac{t_\infty}{a + bt_\infty} = \frac{t_\infty}{bt_\infty} = \frac{1}{b} \quad (6)$$

3.2. Experimental data analysis

To optimize the process, five common parameters affecting the removal rate of a Fenton-like process and adsorption process were studied. Various parameters including initial 1-Na concentrations, FeOOH dosages, PMS concentrations, pH and retention time were

examined and presented with the linear plot of $t / C/C_0$ vs. t and the kinetic constants under various reaction conditions.

The effect of PMS dosage ranging from 0.125–1 mM is illustrated in Fig. 1. It is found that both the initial rate k_i and removal peaked at 0.75 mM, while further increase in [PMS] would result in a sharp drop in rate and removal. In the increasing phase, more PMS could provide more oxidants for 1-Na removal, however the excess of PMS could lead to self-dissociation, reducing the available reactive species [22,23]. Also, other factors such as FeOOH becomes limiting when [PMS] is the only increasing parameter.

Fig. 2 shows the effect of FeOOH (1–4 g) for 1-Na degradation. The removal is expected to increase with the dosage, and k_i shows an increasing trend towards increasing FeOOH dosage as well. More FeOOH could provide more reaction sites for adsorption and PMS activation to take place [15]. Further increase of FeOOH dosage beyond 3 g did not result in significant improvement. One possible explanation is that the excess FeOOH could block the passage of UV rays and reduce the available photons reaching the catalysts and reactants. There are two peaks obtained for k_i curve. The first peak is possibly attributed to the fast initial catalysis, where the second peak is due to the enhanced adsorption by excess FeOOH.

[1-Na] ranging from 0.015 to 0.3 mM were used to study the effect as shown in Fig. 3. The removal is negatively correlated to [1-Na], where higher concentration of 1-Na would result in decreased removal efficiency. The rate k_i however increases with [1-Na] until 0.15 mM then kept constant at high rate. The rate is faster with higher concentrations of 1-Na as more reactants are available, and the reaction is more vigorous. However, as presented, a faster rate does not result in a higher removal, because the radical source, catalyst, and light intensity are all constrained for the fair test. This however can be easily overcome by increasing the [PMS], [FeOOH] and/or [photons] in practice.

The pH levels appear to have a significant impact on removal (Fig. 4). The theoretical removal (C_∞/C_0) has dropped significantly with increasing pH, and the initial rate k_i is optimal at pH around 3, and declined beyond pH 3. It is reported that at lower pH, iron oxides are more soluble, such that Fe(III) is dissociated into aqueous phase, enhancing the homogeneous activation of PMS. Moreover, the photons could activate FeOOH into Fe^{2+} , where Fe^{2+} was able to activate PMS into sulfate radicals [15].

Fig. 5 shows the effect of retention times to the removal performance, and both k_i and removal were best at 15-min retention, with around 80% removal achieved. Unlike adsorption or a complete mixed reactor, where a longer retention time can usually improve the removal performance; longer retention time in a column reactor however does not

always secure a better removal. This is because the “hot zone” in a column type reactor may located (or limited) at certain depth or region instead of the full column, so no strong link between removal and retention time is observed. Based on these results, the five parameters, [PMS], FeOOH dosage, [1-Na], pH and retention time have shown effects on 1-Na degradation in the system, such that these parameters will be added to the prediction model.

3.3. 1-Na degradation pathway

The oxidation by-products in the process were identified by LCMS and GCMS, and are presented in Scheme 1 and the data are presented in Table S2. The major intermediate products identified at time intervals 25 and 35 min are 1,4-naphthaquinone (4) and 1,2-naphthaquinone (7), which are yellowish compound as observed in the reaction mixture. The concentration of 1,4-naphthaquinone (4) and 1,2-naphthaquinone (7) were increased towards the end of reaction, suggesting that they are accumulated in the system. The oxidation of an aromatic ring occurs exclusively via OH adduct, followed by addition of O_2 [24]. Similar reactions were observed here, where compounds (2) and (4) are the OH adduct products, subsequently oxidized into compounds (4) and (7). Other compounds (5 and 6) were also detected in trace amount, where C–C bonds were dissociated, resulting in ring opening products, possibly by direct photolysis.

At the end of reaction ($t = 60$ min), different phenolic compounds (9–11) were identified, showing that the system effectively degraded the two-ring-aromatics into smaller compounds, which has lower molecular weight and less persistent in the environment. The formation of compounds (9–11) is via alkylation process, where the alkyl group is added or substituted onto the aromatic ring. Other studies have reported that 2-rings compounds may form dimer of 4-rings [23,25], however it is not detected in this study, as the larger compounds are expected to be adsorbed onto the catalyst surface, such that the samples collected at the outlet contains only compounds with less carbon. In practice, the products can be mineralized into carbon dioxide and water when the process is allowed to continue with properly selected dosages of PMS, catalyst and UV.

3.4. Multiple linear regression for performance prediction

To develop the prediction model for this process, 21 sets of observations (presented in Table 1). Five variables, initial 1-naphthol concentration (X_1), FeOOH dosage (X_2), PMS concentration (X_3), and pH (X_4) and the retention times, Retention Time (X_5) were used. The

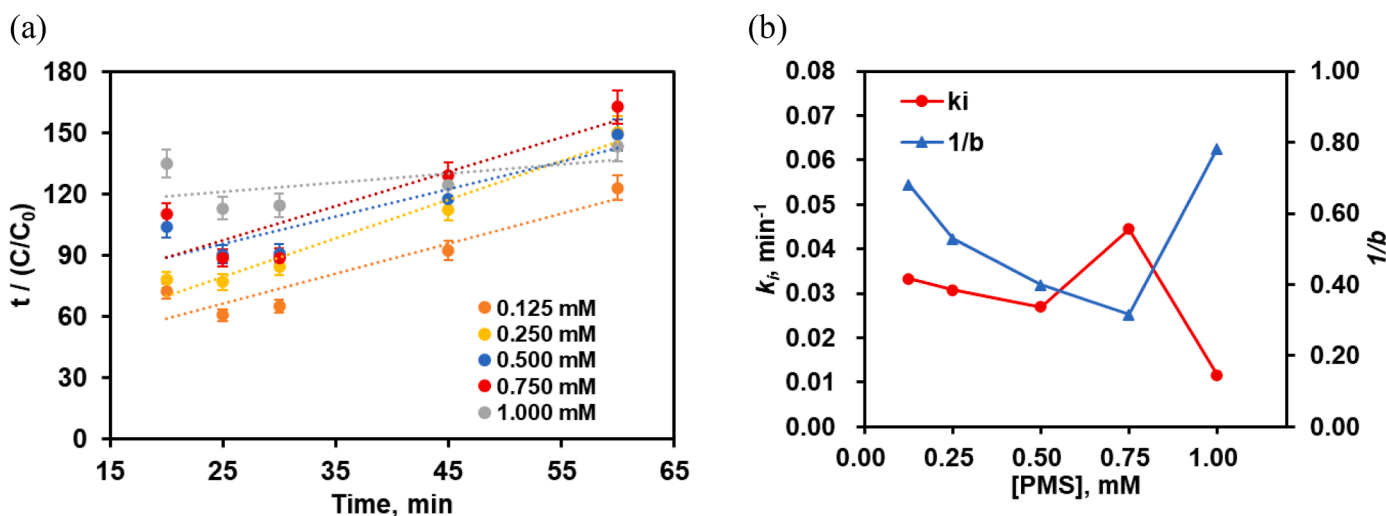


Fig. 1. (a) Degradation curve and (b) Kinetic constants of 1-Na removal under different PMS concentration. (conditions: [1-Na] = 0.15 mM; FeOOH = 3 g; pH = 3.4; Retention time = 15 min).

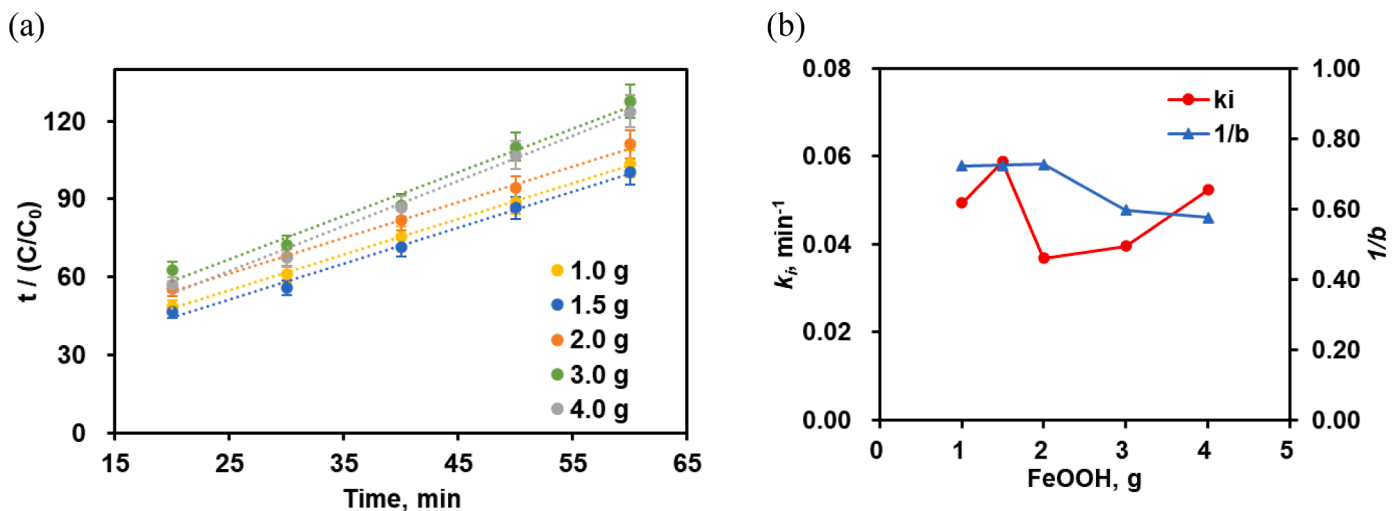


Fig. 2. (a) Degradation curve and (b) Kinetic constants of 1-Na removal under different FeOOH dosages. (conditions: [1-Na] = 0.15 mM; [PMS] = 0.75 mM; pH = 3.4; Retention time = 15 min).

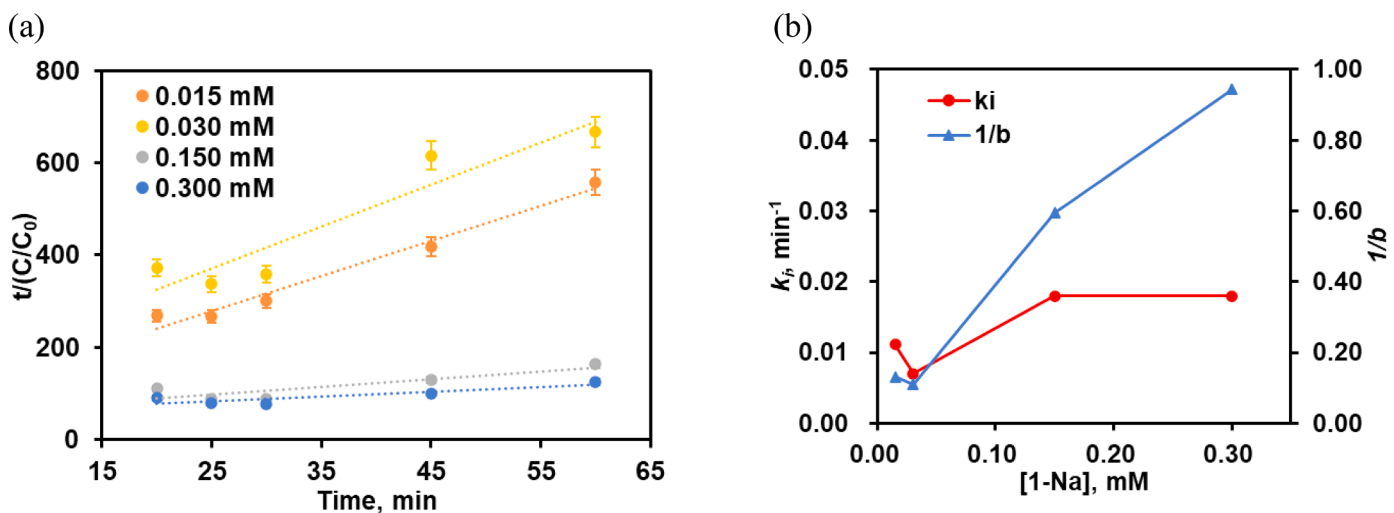


Fig. 3. (a) Degradation curve and (b) Kinetic constants of 1-Na removal under different initial [1-NP]. (conditions: FeOOH = 3 g; [PMS] = 0.75 mM; pH = 3.4; Retention time = 15 mins).

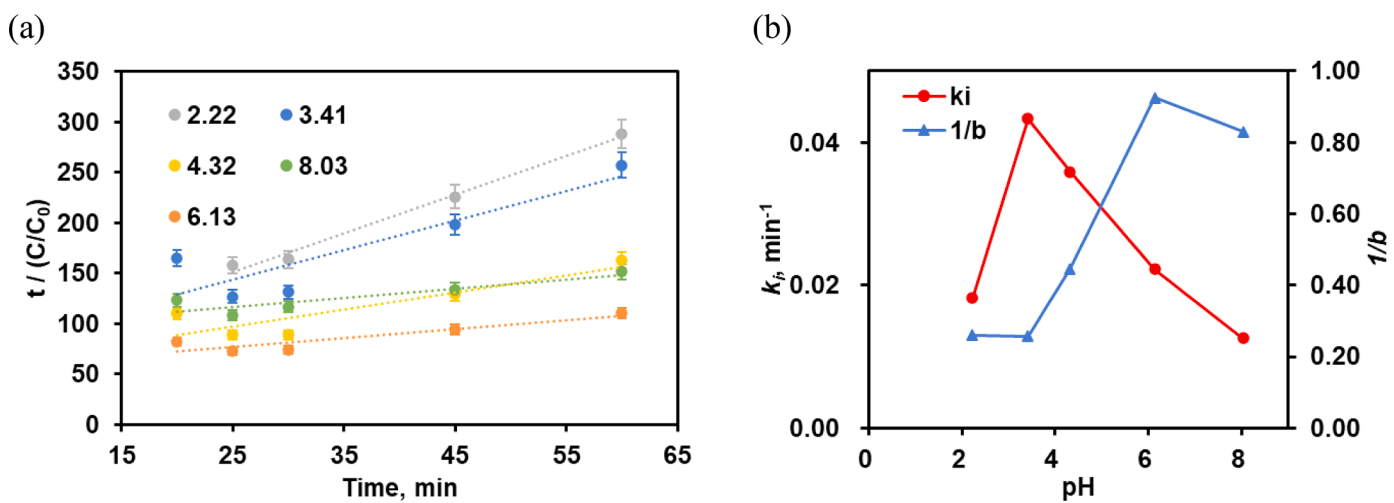


Fig. 4. (a) Degradation curve and (b) Kinetic constants of 1-Na removal under different initial pH levels. (conditions: [1-Na] = 0.15 mM; FeOOH = 3 g; [PMS] = 0.75 mM; Retention time = 15 min).

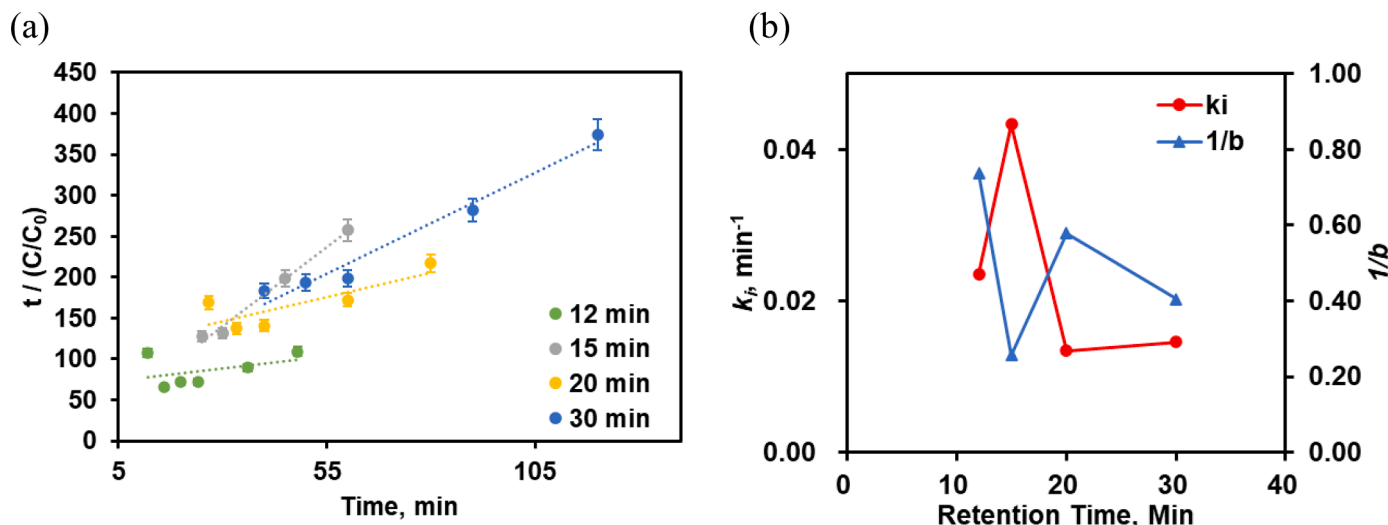


Fig. 5. (a) Degradation curve and (b) Kinetic constants of 1-Na removal under different retention times. (conditions: [1-Na] = 0.15 mM; FeOOH = 3 g; [PMS] = 0.75 mM; pH = 4.32).

Table 1
Experimental results.

Observation	Variables					Response
	X ₁ [1-Na], mM	X ₂ FeOOH, g	X ₃ [PMS], mM	X ₄ pH	X ₅ Retention Time, min	Y A
1	0.15	2	0.25	4.31	15	0.72
2	0.15	2	0	4.32	15	0.77
3	0.015	3	0.75	3.41	15	0.09
4	0.03	3	0.75	3.47	15	0.11
5	0.15	3	0.75	3.41	15	0.37
6	0.3	3	0.75	3.41	15	0.48
7	0.15	0.5	0.25	4.32	15	0.55
8	0.15	1	0.25	4.32	15	0.58
9	0.15	1.5	0.25	4.32	15	0.60
10	0.15	4	0.25	4.32	15	0.48
11	0.15	3	0.125	4.44	15	0.49
12	0.15	3	0.25	4.42	15	0.40
13	0.15	3	0.5	4.46	15	0.40
14	0.15	3	1	4.6	15	0.38
15	0.15	3	0.75	2.22	15	0.21
16	0.15	3	0.75	3.41	15	0.23
17	0.15	3	0.75	4.32	15	0.37
18	0.15	3	0.75	6.13	15	0.54
19	0.15	3	0.75	8.03	15	0.40
20	0.15	3	0.75	3.41	12	0.44
21	0.15	3	0.75	3.41	30	0.32

response Y is selected to be C_{60}/C_0 (denoted as A), which represents the concentration of 1-Na in the system at the end of reaction.

The main effects of individual variables, their second-order effects, and two-way interactions were all examined. pH (X_4) was found to be reciprocally correlated such that the term $1/X_4$ was also included as a regressor. In a full model, all factors summing to a total of 20 terms, shall be included. However, it may be statistically inappropriate as some of the terms are not significant to the response. Therefore, the correlation test was conducted to test the relationship between the response Y (A) and all regressors. The first- and second-order, and the interaction effects were determined by Pearson's correlation test and the variables showing statistical significance are listed in Table 2. The Pearson correlation coefficient (r) is a commonly used measurement for the linear dependence between two variables, where it is defined as a positive correlation if r is close to 1; and negative correlation if r is close to -1. No relationship could be indicated if r is close to 0. The p values in the Pearson test suggest the significance of the r value, and only variables

Table 2
Pearson correlation matrix.

Variables		r	p	Significance
1-Na	X ₁	0.498	0.02	*
FeOOH	X ₂	-0.515	0.01	**
PMS	X ₃	-0.684	<0.0001	**
1/pH	$1/X_4$	-0.482	0.02	*
FeOOH	X ₂ ²	-0.508	0.01	**
PMS	X ₃ ²	-0.625	<0.0001	**
FeOOH : PMS	X ₂ × ₃	-0.7	<0.0001	**
1-Na : pH	X ₁ × ₄	0.576	<0.0001	**

Notes: * Significance level at 0.05; ** Significance level at 0.01.

with $p < 0.05$ will be included in the next steps.

According to the results, variables X_1 , X_2 , X_3 , $1/X_4$, second-order X_2^2 , X_3^2 , and interactions $X_2 \times X_3$, $X_1 \times X_4$, have p -values smaller than 0.05, suggesting a significant correlation to the response, and the variable X_5 has shown no statistical correlation with the response in all tests and therefore was not included in the model. A quadratic polynomial regression including the above variables is then proposed as shown in Eq. (7) and the result of the analysis and parameters statistical analysis are presented in Tables 3a and 3b.

$$Y = \beta_0 + \sum_{i=1}^k \beta_i X_i + \sum_{i=1}^k \beta_{ii} X_i^2 + \sum_{i=1}^k \sum_{j=1}^k \beta_{ij} X_i X_j \quad (7)$$

Where Y represents the response (A), X_i ($i = 1$ to k) represents the independent variables, β_i is the first-order regression coefficients; β_{ii} is the second-order regression coefficient; β_{ij} is the coefficient of interaction between factors i and j ; and β_0 is a constant term [26,1].

Since the regression coefficients proposed are all in different measurement units, a direct comparison is not valid [27]. A standardized model with standardized regression coefficients is therefore included to

Table 3a
ANOVA for proposed regression model.

Analysis of Variance	Sum of squares	DF	Mean Square	F	P-value
Regression	0.520	8	0.065	8.090	0.001
Residual	0.096	12	0.008		
Total	0.617	20			
R ² =0.844	Adj. R ² = 0.739				

Table 3b
Statistical analysis of model parameters for the proposed regression model.

	Unstandardized Coefficients	Standard Error	Standardized Coefficients	<i>t</i>	<i>p</i> -value	Lower boundary 95% Confidence Interval	Upper boundary
β_0	1.022	0.490		2.087	0.059	-0.045	2.090
β_1	1.652	1.052	0.492	1.571	0.142	-0.639	3.944
β_2	-0.087	0.220	-0.402	-0.396	0.699	-0.566	0.392
β_3	-1.772	1.431	-2.913	-1.239	0.239	-4.889	1.345
$B_{1/4}$	-0.971	0.797	-0.353	-1.218	0.247	-2.708	0.766
β_{22}	-0.017	0.029	-0.345	-0.597	0.561	-0.079	0.045
β_{33}	0.192	0.457	0.314	0.420	0.682	-0.805	1.189
β_{23}	0.446	0.578	2.436	0.771	0.455	-0.813	1.704
β_{14}	-0.051	0.279	-0.075	-0.184	0.857	-0.658	0.556

eliminate the problem of different variable units (mM, g. etc.) and provide a direct comparison on the relative significance between the variables. Such that it could be interpreted that [PMS] has the best effect on the removal, increasing one unit of PMS could reduce *A* by 2.913, followed by FeOOH dosage (-0.402) and 1/pH (-0.353). The interaction between FeOOH dosage and [PMS] has the negative effect on the treatment capacity, whereas increasing one unit of FeOOH*PMS results in 2.436 of increase in *A* (poorer removal).

Based on the *p*-value of the regression (0.001), the model has a strong correlation to the experimental data. The regression has an overall R-square of 0.844, suggesting that more than 84% of the data could be predicted by the proposed model, which is amongst the top compared to other similar prediction models (R^2 ranging from 0.555 to 0.835) [28, 29]. A plot of predicted *A* and experimental *A* shown in Fig. 6 has demonstrated the adequate agreement of the regression results and observed results

3.5. Model validation

The predictive ability and accuracy of developed models were verified. 12 additional sets of tests including all mentioned variables were conducted to obtain data for validation. The data were summarized and presented in Table S1. The capacity *A* were calculated using the developed model, where the experimental *A* and predicted *A* is compared and shown in Fig. 7a. Approximately 75% of the predicted *A* falls within $\pm 10\%$ of the experimental *A*, and 92% within $\pm 20\%$. The remaining falls within $\pm 25\%$ of the experimental value. Previous studies

demonstrated that predicted values should be rigidly within $\pm 20\%$ of the measured values [20], which well justified that the developed models could accurately predict the capacity of the reactor.

To further validate the model, a two-tailed T-test was used to determine the differences between the means of predicted and experimental *A*. The t_{value} is 1.208, which is less than the $t_{0.05, 11} = 2.20$, indicating that it is failed to reject the null hypothesis ($m_1 - m_2 = 0$), and the mean difference between the predicted and experimental value is insignificant. In addition, the *p*-value is 0.252, which is larger than 0.05, suggesting that the means of predicted *A* has no obvious difference from the experimental *A*. Internal evaluation was also carried out to validate the developed model as shown in Fig. 7b. The R^2 of the predicted removal vs. experimental removal is 0.948, demonstrating a precise prediction.

3.6. Analysis of response surface plot and process optimization

Response surface plots for *A* with different parameters were conducted to explore the relationship among all variables and response, and three-dimensional figures were used to visualize the interactions as illustrated in Fig. 8, where darker color represents better removal. The interaction effect between [1-Na] (X_1) and pH (X_4) is shown in Fig. 8a. At lower pH and lower initial [1-Na] concentration, better removal efficiency (lower *A*) is observed. Similar trend is revealed for FeOOH dosage (X_2) and pH (X_4), (Fig. 8b), where a lower pH level has positive effect on removal at all FeOOH dosage, however the performance does not increase at higher FeOOH dosage. A plausible explanation is that the

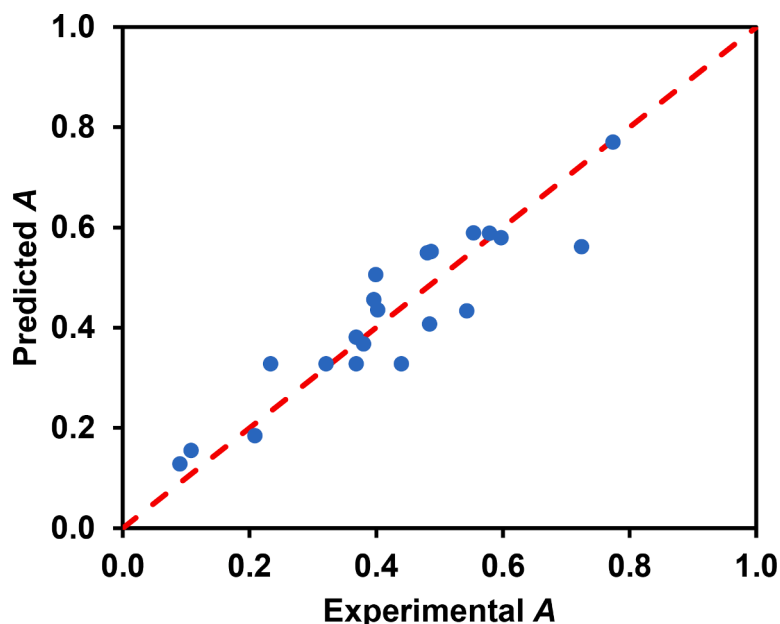


Fig. 6. Predicted *A* vs. Experimental *A*.

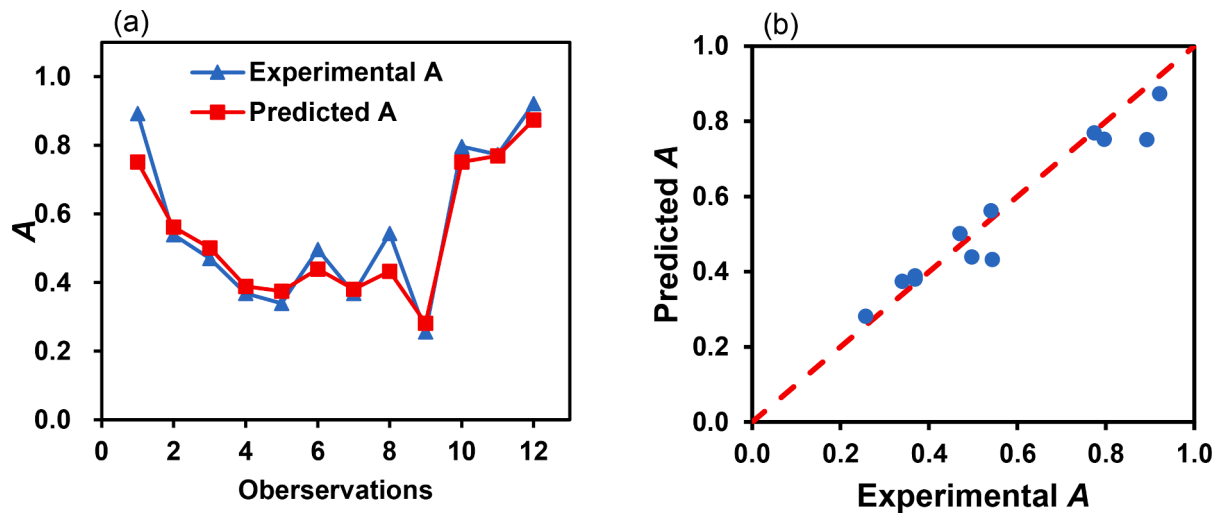


Fig. 7. Validation of the model: predicted and experimental values of A.

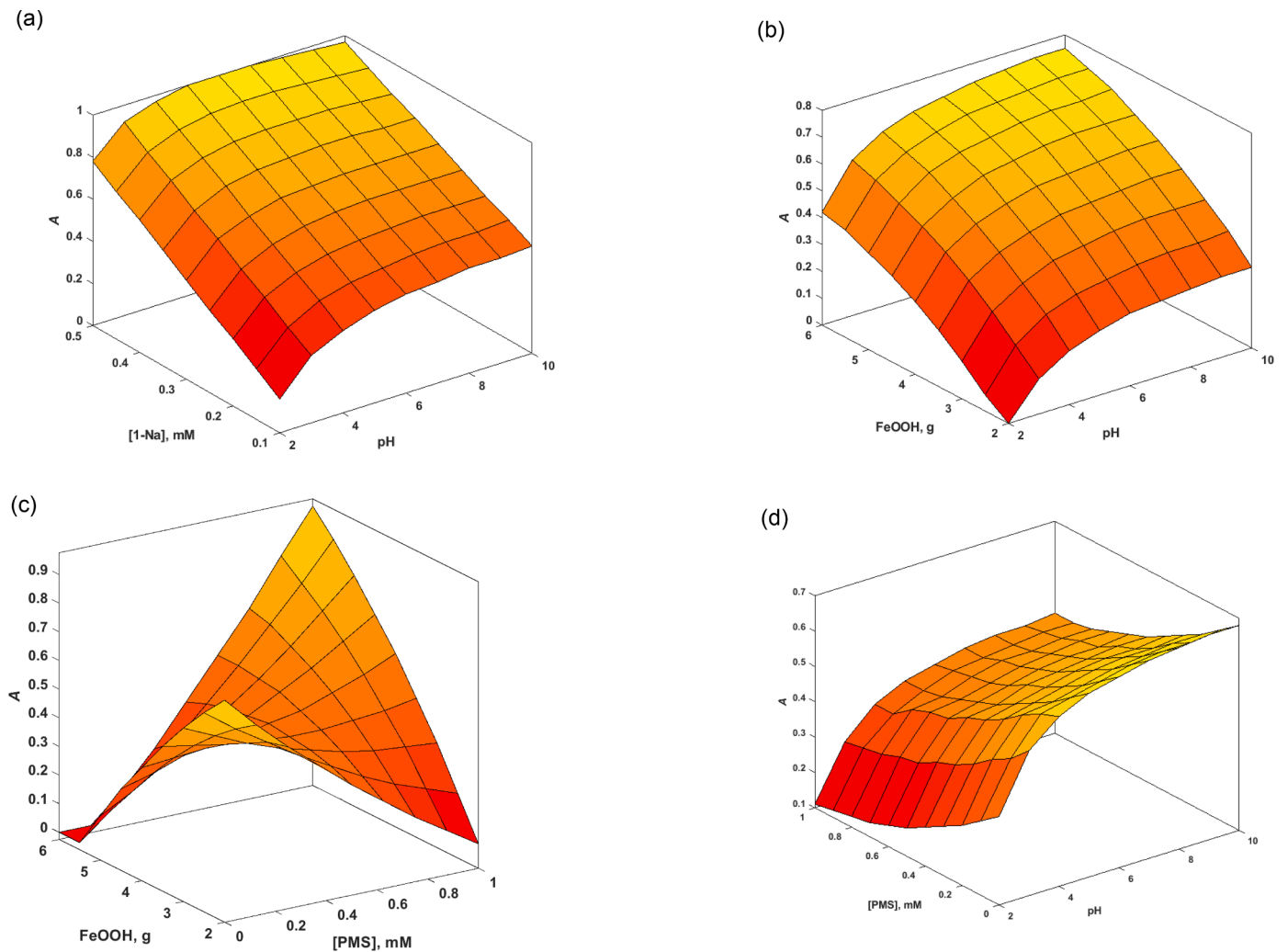


Fig. 8. Response surface plots for A. (a) The effect of initial [1-Na] (X_1) and pH (X_4). (conditions: $FeOOH = 3\text{ g}$; $[PMS] = 0.75\text{ mM}$); (b) The effect of $FeOOH$ dosage (X_2) and pH (X_4). (conditions: $[1-Na] = 0.15\text{ mM}$; $[PMS] = 0.75\text{ mM}$). (c) The effect of $FeOOH$ dosage (X_2) and initial PMS concentration (X_3). (conditions: $[1-Na] = 0.15\text{ mM}$; $pH = 4.32$); (d) The effect of initial PMS concentration (X_3) and pH (X_4). (conditions: $[1-Na] = 0.15\text{ mM}$; $FeOOH = 3\text{ g}$).

interacted bias resulting from the imperfect parameter ranges selected for model development. This problem could be justified by the optimization result by contour plots (to be introduced in next part). Quadratic relationships are observed from interactions between FeOOH dosage (X_2) and [PMS] (X_3) (Fig. 8c). The steep increase in A at both ends suggests that when both FeOOH and PMS are too low or too high, the reaction becomes futile. Otherwise, a steep decrease in A is observed, suggesting that either higher FeOOH dosage with lower [PMS], or higher [PMS] with lower FeOOH dosage could favor the reaction. Fig. 8d shows the relationship between [PMS] (X_3) and pH (X_4). It is noticed that the performance is better at lower pH for any [PMS], and a better removal at higher [PMS] at all pH, since more oxidants could be produced with more PMS present.

To predict the optimized parameter of the process, the capacity A was calculated using the proposed model at a wider range of [PMS] and FeOOH dosages, and the contour plots were overlaid and produced as shown in Fig. 9. The shaded regions represent the performance of the reactor at [PMS] = 0–3 mM and pH = 2–10; and the contour lines represent the performance at FeOOH = 0–6 g and pH = 2–10. Darker colours are the regions with better performance. By overlaying the two contour plots, the optimal region of the reaction for all three variables could be examined, unlike traditional optimization process, which only includes one factor at a time, and the interaction between factors were usually omitted. Based on the overlaid contour plots, the optimal region occurs at pH 2–2.5; [PMS] = 1.2–1.4 mM; and FeOOH 2.75–3 g.

Two sets of additional experiments were carried out under the optimal conditions: (1) [1-Na] = 0.15 mM; FeOOH = 3 g; [PMS] = 1.2 mM; pH = 2.3; and (2) [1-Na] = 0.15 mM; FeOOH = 2.75 g; [PMS] = 1.4 mM; pH = 2.5 to verify the agreement of the results obtained from the contour plots analysis. It was found that the experimental A (0.199 and 0.122) were in resemblance to the predicted A (0.172 and 0.107) with around 15% error, which is because the optimal parameters cited

by overlaid approach were outside the original examined range when developing the model. These results also showed that the optimization approach by using contour plots is superior to the conventional stepwise screening, as the former can optimize different variables at the same time, and the results obtained has the best results ever in this study.

4. Conclusion

A kinetic model was proposed for this system, with kinetic constants k_i and $1/b$ to predict the initial rate and removal capacity. The reaction pathway was proposed based on the mass spectrometry results. On the basis of 21 sets of experimental data, a polynomial linear model with four variables ([1-Na], FeOOH dosage, [PMS] and pH) was proposed to predict the performance of the simultaneous AOP and adsorption by the specialized column reactor. The results show that the model has good reproducibility [$R^2 = 0.844$], and no statistically significant difference was discovered between the experimental and predicted values based on the T-test conducted. The validation results showed that 92% of the predicted values fell within $\pm 20\%$ of the experimental values, demonstrating that the regression model has accurate prediction and could be used to predict the performance of the reactor. Three-dimensional plots were used to visualize the effect and interaction between variables. The process is further optimized based on the overlaid contours resulted from the 3-D plots and concluded that the conditions for the best performance of this reactor is at pH 2–2.5; [PMS] = 1.2–1.4 mM; and FeOOH 2.75–3 g, respectively.

Funding information

The Hong Kong Polytechnic University Research Grant [3-RAAE].

Has no involvement in the experimental design, analysis, data interpretation and writing of the report.

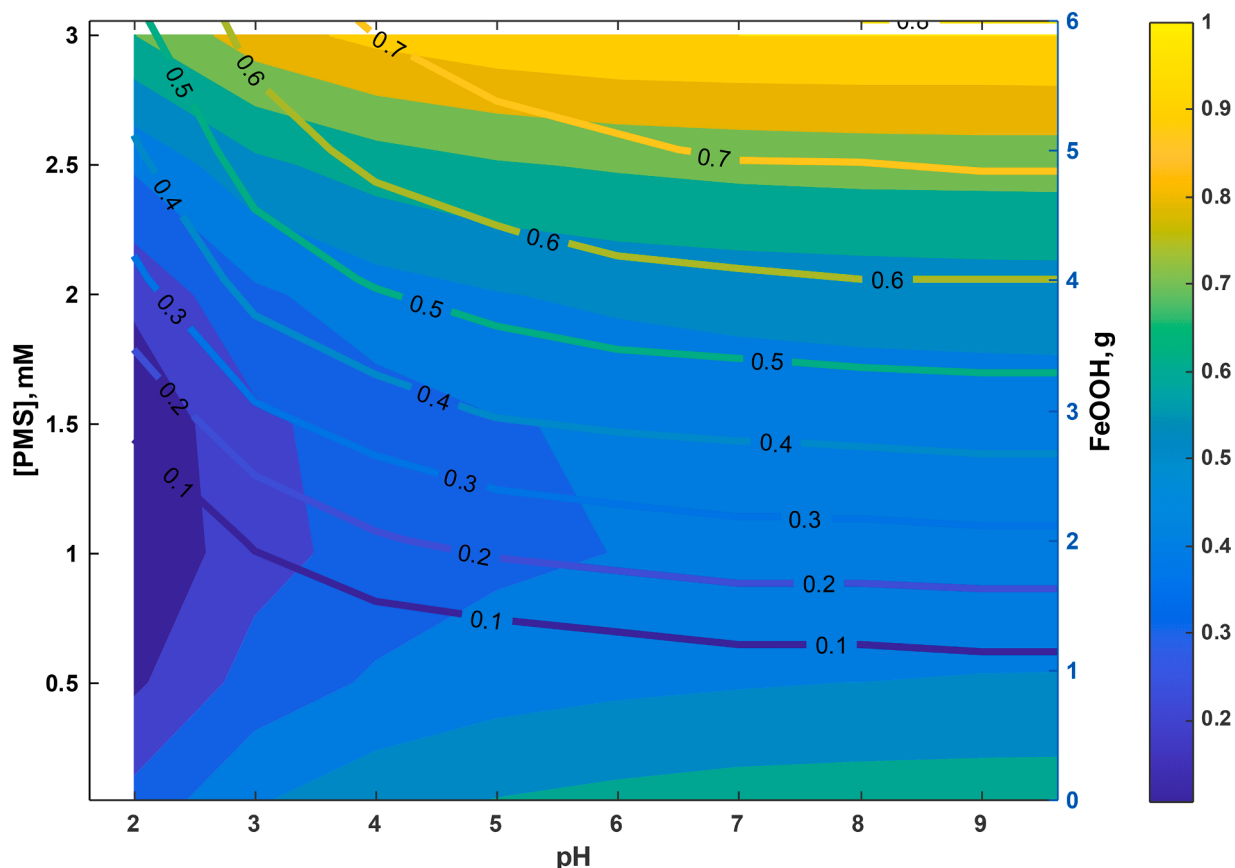
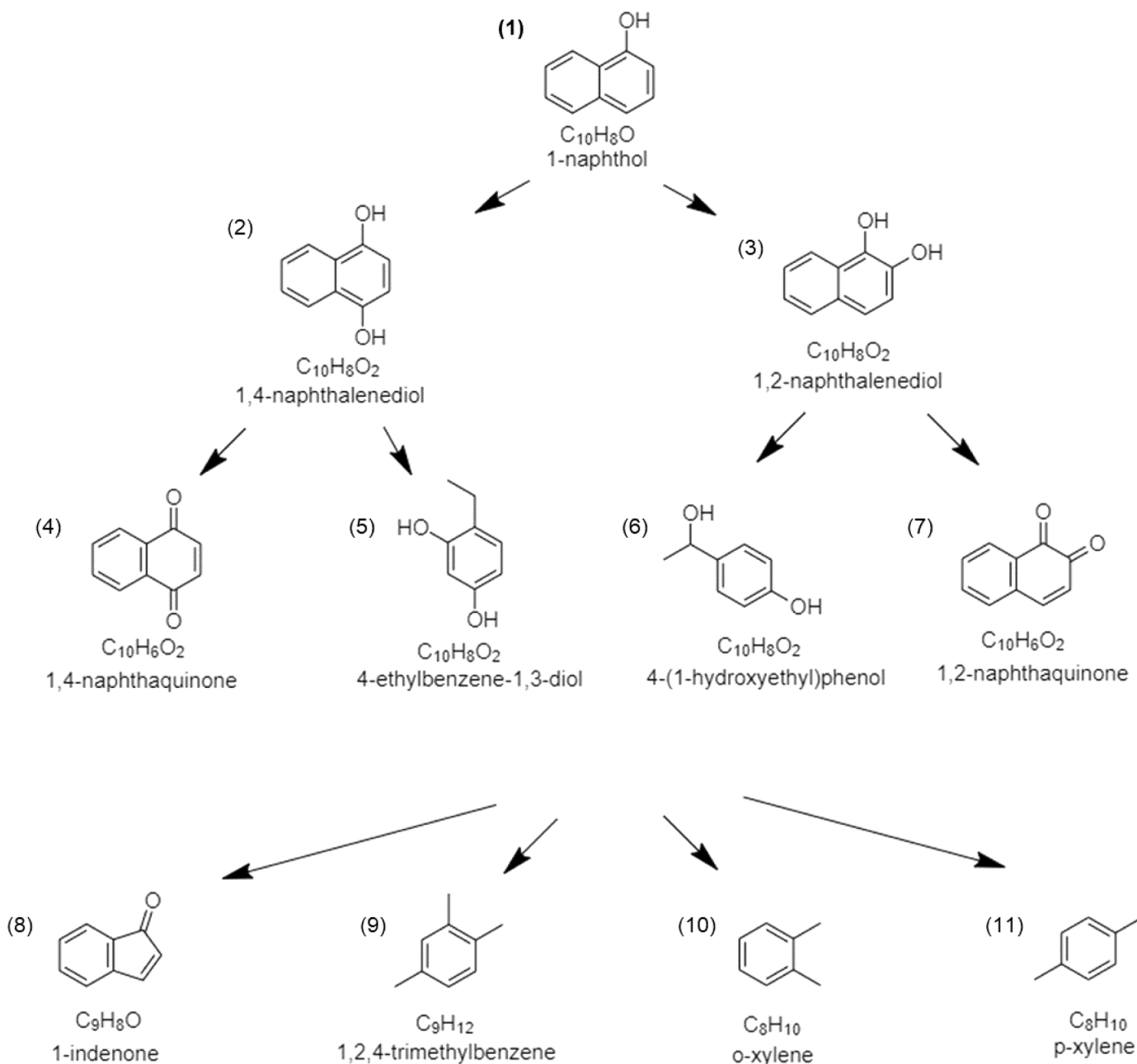


Fig. 9. Contour plots for optimal region. (conditions: [1-Na] = 0.15 mM).



Scheme 1. Proposed 1-naphthol degradation pathway under the system.

Supporting information

Figure S1. Experimental setup; Table S1. Data for validation experiment; Table S2. MS data.

Declaration of Competing Interest

The authors declare that they have no known competing financial interests or personal relationships that could have appeared to influence the work reported in this paper.

Acknowledgement

This work was supported by the Hong Kong Polytechnic University [Research Grant 3-RAAE].

Supplementary materials

Supplementary material associated with this article can be found, in the online version, at [doi:10.1016/j.cej.2022.100395](https://doi.org/10.1016/j.cej.2022.100395).

References

- [1] W. Hu, X. Min, X. Li, J. Liu, H. Yu, Y. Yang, J. Zhang, L. Luo, L. Chai, Y. Zhou, Enhanced degradation of 1-naphthol in landfill leachate using *Arthrobacter* sp, *Environ. Technol.* 40 (7) (2019) 835–842, <https://doi.org/10.1080/09593330.2017.1408695>.
- [2] G. Zhao, J. Li, X. Wang, Kinetic and thermodynamic study of 1-naphthol adsorption from aqueous solution to sulfonated graphene nanosheets, *Chem. Eng. J.* 173 (1) (2011) 185–190, <https://doi.org/10.1016/j.cej.2011.07.072>.
- [3] X.-Q. Liu, H.-S. Ding, Y.-Y. Wang, W.-J. Liu, H. Jiang, Pyrolytic temperature dependent and ash catalyzed formation of sludge char with ultra-high adsorption to 1-naphthol, *Environ. Sci. Technol.* 50 (5) (2016) 2602, <https://doi.org/10.1021/acs.est.5b04536>.
- [4] EPA. Effluent Guidelines and Standards: Organic Chemicals, Plastics and Synthetic Fibers 40 CFR Part 414, Environmental Protection Agency, Washington DC, 1988.

- [5] D.J. Meeker, B.L. Ryan, B.D. Barr, B.R. Hauser, Exposure to nonpersistent insecticides and male reproductive hormones, *Epidemiology* 17 (1) (2006) 61–68, <https://doi.org/10.1097/01.ede.0000190602.14691.70>.
- [6] A. Renglin, A. Olsson, C.A. Wachtmeister, A. Önfelt, Mitotic disturbance by carbaryl and the metabolite 1-naphthol may involve kinase-mediated phosphorylation of 1-naphthol to the protein phosphatase inhibitor 1-naphthylphosphate, *Mutagenesis* 13 (4) (1998) 345–352.
- [7] W. Zhang, C. Hong, B. Pan, Z. Xu, Q. Zhang, L. Lv, Removal enhancement of 1-naphthol and 1-naphthylamine in single and binary aqueous phase by acid–basic interactions with polymer adsorbents, *J. Hazard. Mater.* 158 (2) (2008) 293–299, <https://doi.org/10.1016/j.jhazmat.2008.01.079>.
- [8] W. Zhang, Z. Xu, B. Pan, Q. Zhang, Q. Zhang, W. Du, B. Pan, Q. Zhang, Cooperative effect of lateral acid–base interaction on 1-naphthol/1-naphthylamine binary adsorption onto nonpolar polymer adsorbents, *Sep. Purif. Technol.* 55 (2) (2007) 141–146, <https://doi.org/10.1016/j.seppur.2006.11.011>.
- [9] D. Zhao, L. Zhao, C.S. Zhu, X. Shen, X. Zhang, B. Sha, Comparative study of polymer containing beta-cyclodextrin and -COOH for adsorption toward aniline, 1-naphthylamine and methylene blue, *J. Hazard. Mater.* 171 (1–3) (2009) 241–246, <https://doi.org/10.1016/j.jhazmat.2009.05.134>.
- [10] W. Zhang, C. Hong, B. Pan, Z. Xu, Q. Zhang, L. Lv, Removal enhancement of 1-naphthol and 1-naphthylamine in single and binary aqueous phase by acid–basic interactions with polymer adsorbents, *J. Hazard. Mater.* 158 (2–3) (2008) 293–299, <https://doi.org/10.1016/j.jhazmat.2008.01.079>.
- [11] J. Hu, D. Shao, C. Chen, G. Sheng, X. Ren, X. Wang, Removal of 1-naphthylamine from aqueous solution by multiwall carbon nanotubes/iron oxides/cyclodextrin composite, *J. Hazard. Mater.* 185 (1) (2011) 463–471, <https://doi.org/10.1016/j.jhazmat.2010.09.055>.
- [12] W. Zhang, J. Chen, B. Pan, Q. Zhang, Cooperative adsorption behaviours of 1-naphthol and 1-naphthylamine onto nonpolar macroreticular adsorbents, *React. Funct. Polym.* 66 (5) (2006) 485–493, <https://doi.org/10.1016/j.reactfunctpolym.2005.08.017>.
- [13] Y. Cai, X. Wen, Y. Wang, H. Song, Z. Li, Y. Cui, C. Li, Preparation of hypercrosslinked polymers with hierarchical porous structure from hyperbranched polymers for adsorption of naphthalene and 1-naphthylamine, *Sep. Purif. Technol.* 266 (2021), <https://doi.org/10.1016/j.seppur.2021.118542>.
- [14] H.L. So, W. Chu, W. Xu, Photocatalysis of naphthalene by Fe₃O₄/Oxone/UV: simultaneous radical and non-radical pathways, *J. Environ. Chem. Eng.* 9 (2) (2021), 105076, <https://doi.org/10.1016/j.jece.2021.105076>.
- [15] X. Li, Y. Huang, C. Li, J. Shen, Y. Deng, Degradation of pCNB by Fenton like process using α -FeOOH, *Chem. Eng. J.* 260 (2015) 28–36, <https://doi.org/10.1016/j.cej.2014.08.042>.
- [16] X. Qian, M. Ren, Y. Zhu, D. Yue, Y. Han, J. Jia, Y. Zhao, Visible light assisted heterogeneous fenton-like degradation of organic pollutant via α -FeOOH/mesoporous carbon composites, *Environ. Sci. Technol.* 51 (7) (2017) 3993–4000, <https://doi.org/10.1021/acs.est.6b06429>.
- [17] G.B. Ortiz de la Plata, O.M. Alfano, A.E. Cassano, Decomposition of 2-chlorophenol employing goethite as Fenton catalyst. I. Proposal of a feasible, combined reaction scheme of heterogeneous and homogeneous reactions, *Appl. Catal. B* 95 (1) (2010) 1–13, <https://doi.org/10.1016/j.apcatb.2009.12.005>.
- [18] S. Pari, I.A. Wang, H. Liu, B.M. Wong, Sulfate radical oxidation of aromatic contaminants: a detailed assessment of density functional theory and high-level quantum chemical methods, *Environ. Sci. Process. Impacts* 19 (3) (2017) 395–404, <https://doi.org/10.1039/c7em00009j>.
- [19] R. Yuan, S.N. Ramjaun, Z. Wang, J. Liu, Effects of chloride ion on degradation of Acid Orange 7 by sulfate radical-based advanced oxidation process: implications for formation of chlorinated aromatic compounds, *J. Hazard. Mater.* 196 (2011) 173–179, <https://doi.org/10.1016/j.jhazmat.2011.09.007>.
- [20] S.K. Golfinopoulos, G.B. Arhonditsis, Multiple regression models: a methodology for evaluating trihalomethane concentrations in drinking water from raw water characteristics, *Chemosphere* 47 (9) (2002) 1007–1018, [https://doi.org/10.1016/S0045-6535\(02\)00058-9](https://doi.org/10.1016/S0045-6535(02)00058-9).
- [21] S. Chowdhury, P. Champagne, P.J. McLellan, Models for predicting disinfection byproduct (DBP) formation in drinking waters: a chronological review, *Sci. Total Environ.* 407 (14) (2009) 4189–4206, <https://doi.org/10.1016/j.scitotenv.2009.04.006>.
- [22] Y.R. Wang, W. Chu, Degradation of a xanthen dye by Fe(II)-mediated activation of Oxone process, *J. Hazard. Mater.* 186 (2–3) (2011) 1455–1461, <https://doi.org/10.1016/j.jhazmat.2010.12.033>.
- [23] J. Liu, H.L. So, W. Chu, Degradation of 1-naphthylamine by a UV enhanced Fe²⁺/peroxymonosulfate system: a novel pH-dependent activation pathway, *Chem. Eng. J.* 443 (2022), 136299, <https://doi.org/10.1016/j.cej.2022.136299>.
- [24] B. Klotz, R. Volkamer, M.D. Hurley, M.P.S. Andersen, O.J. Nielsen, I. Barnes, T. Imamura, K. Wirtz, K.-H. Becker, U. Platt, T.J. Wallington, N. Washida, OH-initiated oxidation of benzene Part II. Influence of elevated NO concentrations, *Phys. Chem. Chem. Phys.* 4 (18) (2002) 4399–4411, <https://doi.org/10.1039/B204398J>.
- [25] S.M.S. Chauhan, B. Kalra, P.P. Mohapatra, Oxidation of 1-naphthol and related phenols with hydrogen peroxide and potassium superoxide catalysed by 5,10,15,20-tetraarylporphyrinatoiron(III)chlorides in different reaction conditions, *J. Mol. Catal. A Chem.* 137 (1) (1999) 85–92, [https://doi.org/10.1016/S1381-1169\(98\)00079-X](https://doi.org/10.1016/S1381-1169(98)00079-X).
- [26] B. Chen, P. Westerhoff, Predicting disinfection by-product formation potential in water, *Water Res.* 44 (13) (2010) 3755–3762, <https://doi.org/10.1016/j.watres.2010.04.009>.
- [27] A.F. Siegel, Chapter 12 - multiple regression: predicting one variable from several others, in: A.F. Siegel (Ed.), *Practical Business Statistics*, 7th Edition, Academic Press, 2016, pp. 355–418, <https://doi.org/10.1016/B978-0-12-804250-2.00012-2>.
- [28] S. Ghafari, H.A. Aziz, M.H. Isa, A.A. Zinatizadeh, Application of response surface methodology (RSM) to optimize coagulation–flocculation treatment of leachate using poly-aluminum chloride (PAC) and alum, *J. Hazard. Mater.* 163 (2) (2009) 650–656, <https://doi.org/10.1016/j.jhazmat.2008.07.090>.
- [29] C. Karunakaran, S. Narayanan, P. Gomathisankar, Photocatalytic degradation of 1-naphthol by oxide ceramics with added bacterial disinfection, *J. Hazard. Mater.* 181 (1) (2010) 708–715, <https://doi.org/10.1016/j.jhazmat.2010.05.070>.